GCB Bioenergy (2009) **1**, 282–296, doi: 10.1111/j.1757-1707.2009.01019.x

A semimechanistic model predicting the growth and production of the bioenergy crop *Miscanthus* × *giganteus:* description, parameterization and validation

FERNANDO E. MIGUEZ*†, XINGUANG ZHU‡[1], STEPHEN HUMPHRIES§, GERMÁN A. BOLLERO* and STEPHEN P. LONG*‡†

*Department of Crop Sciences, University of Illinois at Urbana-Champaign, 1102 S, Goodwin Ave., Urbana, IL 61801, USA, †Energy Biosciences Institute, Institute for Genomic Biology, 1206 West Gregory Drive, MC-195, Urbana, IL 61801, USA, ‡Department of Plant Biology, University of Illinois at Urbana-Champaign, 1201 W, Gregory Drive, 379 Madigan Lab., Urbana, IL 61801, USA, §ADAS, Woodthorne Wergs Road, Wolverhampton WV6 8TQ, UK

Abstract

Biomass based bioenergy is promoted as a major sustainable energy source which can simultaneously decrease net greenhouse gas emissions. *Miscanthus* × *giganteus* (*M.* × *giganteus*), a C_4 perennial grass with high nitrogen, water, and light use efficiencies, is regarded as a promising energy crop for biomass production. Mathematical models which can accurately predict *M.* × *giganteus* biomass production potential under different conditions are critical to evaluate the feasibility of its production in different environments. Although previous models based on light-conversion efficiency have been shown to provide good predictions of yield, they cannot easily be used in assessing the value of physiological trait improvement or ecosystem processes. Here, we described in detail the physical and physiological processes of a previously published generic mechanistic eco-physiological model, WIMOVAC, adapted and parameterized for *M.* × *giganteus*. Parameterized for one location in England, the model was able to realistically predict daily field diurnal photosynthesis and seasonal biomass at a range of other sites from European studies. The model provides a framework that will allow incorporation of further mechanistic information as it is developed for this new crop.

Keywords: bioenergy, biofuels, crop models, *M.* × *giganteus*, mathematical modeling, Miscanthus, WIMOVAC

Received 17 February 2009; revised version received 16 June 2009 and accepted 21 June 2009

Introduction

The recent interest on the potential of biofuels (Koonin, 2006; Ragauskas *et al*., 2006; U.S.DOE, 2006) to supply energy security, reduce carbon dioxide emissions and support agriculture, demands that the most productive, efficient and environmentally responsible cropping systems are used (Heaton *et al*., 2008). At present ethanol constitutes 99% of the biofuels in the United States and it is mainly derived from maize (*Zea mays* L.) (Farrell *et al*., 2006). Although the use of maize-derived ethanol is expected to increase, cellulosic ethanol will be needed in order to meet the longer-term renewable energy mandate (U.S.DOE, 2006). In addition, when harvesting biomass crops nearly all aboveground plant components can be used for cellulosic ethanol production which can enable much larger quantities of biofuel production compared with grain-derived ethanol (Lewandowski *et al*., 2000). *Miscanthus* × *giganteus*, Greef et Deux. Hodkinson et Renvoize, (Hodkinson & Renvoize, 2001), hereinafter referred to as *M.* × *giganteus*, is a C_4 perennial grass with high yield potential (Heaton *et al*., 2004, 2008), efficient conversion of radiation to biomass (Beale & Long, 1997), efficient use of nitrogen (N) and water (Beale & Long, 1995), which has been extensively researched in Europe (Lewandowski

Correspondence: Fernando E. Miguez, Department of Crop Sciences University of Illinois at Urbana-Champaign. 1102 S. Goodwin Ave., Urbana, IL 61801, USA, e-mail: miguez@illinois.edu

[1]Current address: Plant Systems Biology Group, CAS-MPG Partner Institute of Computational Biology, 342 Yue Yang Road, Shanghai 200031, China

et al., 2000). However, at the moment *M.* × *giganteus* is not commercially produced at large scale in the United States, being limited mostly to experimental plots. Thus, there is a need for the development and parameterization of process-based crop models that can provide reliable predictions of carbon assimilation, growth and yield. Further, it is currently an unimproved crop with significant opportunities for yield improvement via selection, breeding and genetic engineering. A semimechanistic model would provide a framework in which to evaluate potential traits for improvement, ahead of a lengthy breeding program.

Previous semimechanistic models based on light conversion efficiency and temperature thresholds for leaf growth have been shown effective for simulating *M.* × *giganteus* yields (Clifton-Brown *et al*., 2000, 2004; Price *et al*., 2004). These models strongly depend on a parameter which describes the efficiency of the crop in converting radiation to biomass (radiation use efficiency, RUE). Although in these models RUE has been treated as a constant, Clifton-Brown *et al*. (2000, 2004) reported that the value of e_c for *M.* × *giganteus* ranged from 2.4 to 4.2 g MJ^{-1} PAR. These authors recognized that the model depends strongly on RUE and that a more mechanistic model would be more appropriate (Clifton-Brown *et al*., 2001). These models are appealing due to their simplicity but by their design they cannot provide insights into the physiological basis of RUE variation, or growth and the physiology of water use (Demetriades-Shah *et al*., 1992; Reddy, 1995; Loomis & Amthor, 1999).

WIMOVAC is a generic plant production model, based on the key physiological and micrometeorological processes underlying plant production (Humphries & Long, 1995). Here, we describe the model as adapted to the specific crop, *M.* × *giganteus*. The model was parameterized from laboratory physiological measurements and shown to effectively predict diurnal photosynthesis in the field. Biomass partitioning was parameterized from measurements made at one site in England. Finally, we demonstrate the ability of the model to predict biomass accumulation and yield for the same genotype at sites distinct from that used for parameterization.

Description of the model

Macroclimate

The macroclimate data (i.e. light, temperature, relative humidity, rainfall, and wind speed) were obtained from records made at each trial location. Day, time, and latitude were used to determine the solar declination and solar zenith angle. Given the solar constant and atmospheric transmittance, the direct and diffuse solar radiation above canopy were predicted (Norman, 1980) Eqns (A1)–(A5). The air temperature was simulated as a function of daily mean temperature Eqn (A6), range Eqn (A7) and excursion Eqns (A8) and (A9). The parameter h_r in Eqn (A8) was determined experimentally and allowed a time offset between the maximum incident solar radiation and the maximum temperature of simulated days that reflects the localized heat capacity of the surroundings. The model assumed that all rainfall was incident upon the soil surface and wind speed was determined experimentally (2 m above the canopy).

Leaf level photosynthesis

Leaf CO_2 uptake rate (A) was predicted from the steady-state model of Collatz *et al*. (1992) Eqns (A10)–(A14). To mimic decrease in stomatal conductance (g_s) with water stress, a linear relationship was assumed between reduction in g_s Eqns (A15)–(A18) and the decrease of leaf water potential.

Canopy level photosynthesis

The proportion of a canopy that was sunlit and shaded at any point in time was determined based on Norman (1980) and Forseth & Norman (1991). The leaf area of sunlit and shaded leaves and the mean irradiance of these two populations were calculated dynamically Eqns (A20)–(A26). Sunlit leaves were assumed to receive direct (I_{dir}) and diffuse (I_{diff}) solar radiation Eqn (A23) while shaded leaves received diffuse and scattered (I_{scat}) light from other leaves in the canopy Eqn (A24). Total canopy photosynthesis was the sum of the photosynthesis at both the sunlit and shaded leaves, calculated by the equation for leaf CO_2 uptake rate Eqn (A27). The canopy was divided into 10 layers and the proportion of sun and shade leaves, and their radiative conditions computed for each, following the above principles Eqns (A20)–(A34). This multilayer approach is essential in modeling the canopy of *M.* × *giganteus* since it can exceed 3 m in canopy height (Cosentino *et al*., 2007). In most natural canopies, leaves assume a range of orientations in which they may be predominantly horizontal (planophile), vertical (erectophile) or an intermediate mixture. A single parameter, χ (the ratio of the horizontal projection of the ellipsoid to the vertical) was used to describe the shape of the distribution and calculate the canopy extinction coefficient [k, Eqn (A19)].

The instantaneous transpiration for each leaf class within the canopy was calculated following the approach of Penman–Monteith (Monteith, 1973) and using the stomatal conductance for each layer and sunlit/shaded leaf class following Collatz *et al*. (1992) Eqns (A36) and (A37). Transpiration values of both sunlit and shaded leaves at all layers were then summed to give total canopy

water loss. The transpiration and leaf temperature were calculated iteratively considering the interaction between energy balance, photosynthesis and conductance at the leaf surface Eqn (A23) and (A24). Total canopy assimilation, transpiration and conductance were obtained by integrating over individual leaf classes Eqns (A27)–(A37).

Growth, partitioning and allocation

Carbon allocation was determined by dry biomass partitioning coefficients which depend on phenological stages. These phenological stages were controlled by thermal periods defined by the sum of average daily temperatures from the start of the growing season. In this way the fraction of available carbon was allocated to each of the plant structural pools, i.e. leaf, stem, structural root, fine root, and rhizome at the current stage Eqn (A52)–(A60). Thus, by varying these coefficients (−1 to 1), the dynamic source/sink demands of the plant during development were modelled. The total carbon available for growth during a given developmental stage was the total of net photosynthetic assimilation and leaf/storage root remobilization Eqn (A53). The new leaf area, stem or root length was simulated based on allocated carbon resources for each tissue and the specific leaf area, specific stem length, and specific root length, respectively, Eqns (A61)–(A64). New leaf growth was assumed to occur uniformly with respect to height in the canopy. Additionally, new stem growth was associated with an increase in canopy height and new root growth with an increase in root density at a specific soil depth.

Respiration

Respiration (R_{total}), following Penning de Vries (1972), was calculated by assuming that growth respiration was a constant fraction of gross photosynthesis. However, the respiratory cost of maintaining plant structures varied depending on the tissue type and temperature [Eqn (A65); Spain & Keen, 1992].

Soil-plant water relations, surface evaporation, soil heat flux and temperature

An analytical plant water uptake model derived by Campbell (1991) was used to predict water potentials in soil and plant system. This model considered the soil profile as a series of discrete layer slices, each with a characteristic root density, soil water potential and associated resistance. Water would move up or down the profile according to soil conductance to water flow and water potential differences between adjacent slices. Water was assumed to move from the soil, through the plant, to the evaporating surface in the substomatal cavities in response to gradients in water potential. The soil water potential, leaf water potential, transpiration, and stomatal conductance are interdependent and therefore were calculated simultaneously using an iterative process Eqns (A66)–(A76).

The evapo-transpiration model of Penman (1948) and Monteith (1973) were used to predict soil evaporation Eqns (A66)–(A76). This formulation included a soil boundary layer conductance term to give actual rather than potential evaporation and shows the expected reduction in evaporation rate associated with increasing canopy leaf area. The conductive heat transfer and water flux in soil followed simple diffusion, as in Chung & Horton (1987). Boundary conditions, latent and sensible heat fluxes were calculated using an energy balance approach through an iterative procedure Eqns (A77)–(A80).

Parameterization of WIMOVAC for *M.* × *giganteus*

The C_4 photosynthesis parameters (Table 1) were obtained from Collatz *et al*. (1992) and validated using data from Naidu *et al*. (2003) and Beale *et al*. (1996). Several studies have shown that *M.* × *giganteus* is able to attain high photosynthetic potential at low temperatures (Beale & Long, 1995; Beale *et al*., 1996; Naidu *et al*., 2003). The default values in Collatz *et al*. (1992) provided a satisfactory fit ($R^2 = 0.99$) when this model was used to predict the temperature response studied in Naidu *et al*. (2003) as shown in Fig. 1.

The length of the growing season was assumed to span from the last frost in the spring until the first frost in the fall (Price *et al*., 2004). Phenological stages followed typical phases in grasses (Cao & Moss, 1997), including emergence, juvenile stage, floral apex initiation, panicle emergence, anthesis, and end of cycle. Contrary to grain crops, the modeling of the reproductive organ development in

Table 1 Parameters in Collatz *et al*. (1992) photosynthesis model

Parameter description	Value
Initial slope of photosynthetic CO_2 response (k_p, mol $m^{-2} s^{-1}$)	0.7
Maximum Rubisco capacity (V_{max}, μmol $m^{-2} s^{-1}$)	39
Initial slope of photosynthetic light response (α, mol mol^{-1})	0.04
Leaf respiration rate (Rd, μmol $m^{-2} s^{-1}$)	0.8
Curvature parameter (θ). Gives gradual transition between light limited and carboxylation limited flux	0.83
Curvature parameter (β). Analogous to θ. Describes the co-limitation between flux determined by Rubisco and light and CO_2 limited flux	0.93

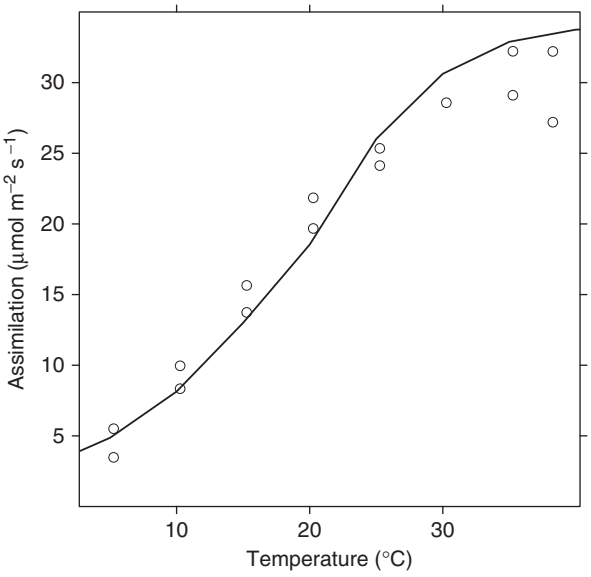

Fig. 1 Observed and simulated assimilation of *M.* × *giganteus*. The open circles are observed data from Naidu *et al*. (2003) and the solid line is simulated using the Collatz *et al*. (1992) model in WIMOVAC ($R^2 = 0.99$).

M. × *giganteus* is of negligible importance. Flowering was predicted to start around 3500 °Cd (degree days; with a base temperature of 0 °C) and the end of the season was around 4000 °Cd (Table 3). At the moment a mechanistic model of leaf senescence is not available, mainly because the relationship between environmental factors which trigger the onset of leaf senescence at different locations has not been elucidated. In addition, there are limited data available on the decay of harvestable biomass after peak yield, which are needed to parameterize a leaf senescence and biomass decay model (Hastings *et al*., 2009). The leaf was assumed to start senescing at 2000 °Cd in the United Kingdom and 4000 °Cd in southern Italy based on two experiments (Beale & Long, 1997; Cosentino *et al*., 2007), with intermediate values for other locations using a simple linear interpolation based on latitude (i.e. senescence thermal time = latitude × −86.7 + 6507). It was further assumed that 60% of the mass of a leaf is reabsorbed during its senescence. Leaf area index (LAI, m^2 leaf m^{-2} soil) was simulated by assuming a constant specific leaf area (Sp_{leaf}) Eqn (A63) of 65 g m^{-2} and the canopy was simulated using 10 layers.

Initial values for coefficients for dry biomass partitioning were determined empirically from the measurements of Beale & Long (1997) with a mature (third year) *M.* × *giganteus* plots in SE England (Table 2). However, this experiment did not provide the complete information needed to estimate the dry biomass partitioning coefficients (Table 2). Additional data from Beale & Long (1995) suggested that initially carbohydrates are partitioned in equal proportions to root, leaf and stem components. With this additional information, the dry biomass partitioning coefficients were obtained (Table 3). This parameterization showed an acceptable agreement between model simulations and observed dry biomass (Fig. 2) in Beale & Long (1997). This model was then tested, without further parameter adjustment, against data for the same genotype at eight study sites elsewhere in Europe (van der Werf *et al*., 1992; Schwarz *et al*., 1994; Danalatos *et al*., 1996, 1998, 2007; Jorgensen, 1996; Foti *et al*., 1996; Clifton-Brown *et al*., 2000). The weather conditions at each location, daily solar radiation, temperature and relative humidity, were obtained either from the individual studies, where reported, or from the World Meteorological Organization (World Meteorological Organization, 2007).

Table 2 Prior information regarding *M.* × *giganteus* dry biomass partitioning at different days during the growing season (DOY, day of the year) from Beale & Long (1997)

	Dry biomass (Mg ha^{-1})			Difference (Mg ha^{-1})			Proportion		
DOY	Rhizome	Stem	Leaf	Rhizome	Stem	Leaf	Rhizome	Stem	Leaf
115	7.2	0	0	–	–	–			
157	6.4	4	3.6	−0.8	4	3.6		0.53	0.47
195	5.6	14.7	5.4	−0.8	10.7	1.8		0.86	0.14
230	9.0	21.1	4.2	3.4	6.4	−1.2	0.35	0.65	
264	10.4	24.2	3.2	1.4	3.1	−1.0	0.31	0.69	
307	9.4	24.2	1.5	−1.0	0	−1.7			
350	10.3	23.1	0	0.9	−1.1	−1.5			

Table 3 *M.* × *giganteus* phenological stages and dry biomass partitioning coefficients. These coefficients are obtained from the calculations in Table 2 and assumptions regarding dry biomass partitioning to roots which were not measured on the Beale & Long (1997) study. Thermal period is the interval for each phenological stage in thermal time units; the first number is the start of the period and the second is the end

Stage	Thermal Period (°Cd)	Leaf	Stem	Rhizome	Root
Emergence	0–525	0.33	0.37	−0.1	0.3
Juvenile	525–1226	0.14	0.85	−0.08	0.01
Induction	1226–1927	0.01	0.63	0.35	0.01
Post-induction	1927–3500	0.01	0.63	0.35	0.01
Flowering	3500–3600	0.01	0.63	0.35	0.01
Post-flowering	3600–4000	0.01	0.63	0.35	0.01

Results and discussion

The predicted photosynthetic CO_2 uptakes of *M.* × *giganteus* at different temperatures correlated well with controlled environment laboratory measurements (Naidu *et al*., 2003) (Fig. 1). Furthermore, the field diurnal CO_2 uptake of Beale *et al*. (1996) was closely simulated for

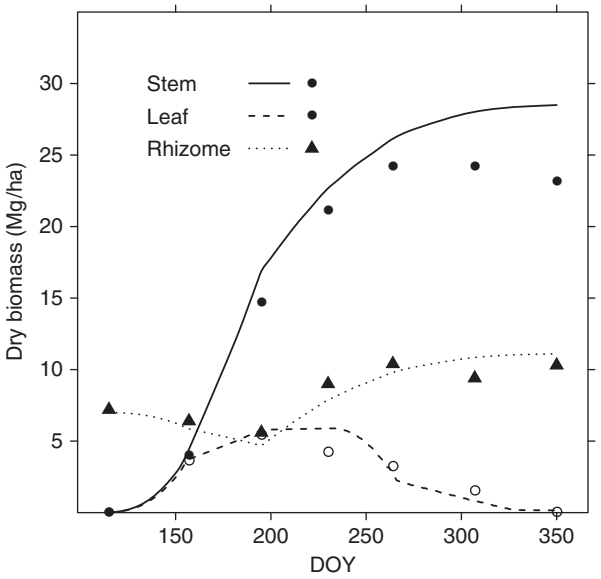

Fig. 2 Observed and simulated *M.* × *giganteus* dry biomass partitioning for data from Beale & Long (1997) through the growing season (DOY, day of the year).

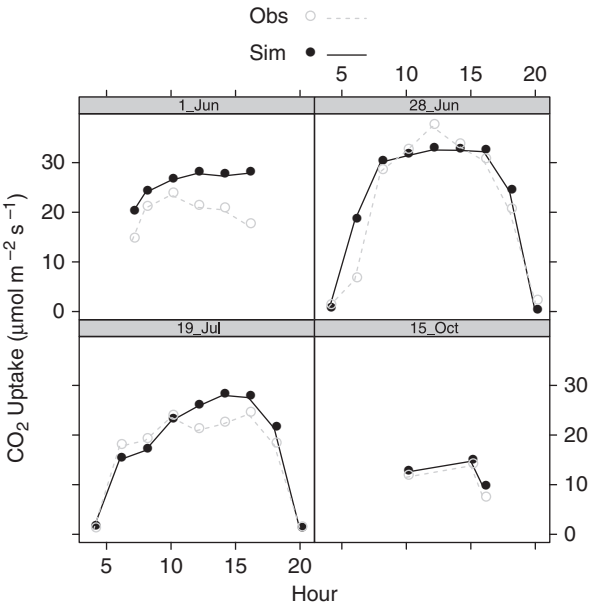

Fig. 3 Observed (open circles) and simulated (closed circles) diurnal carbon dioxide assimilation of *M.* × *giganteus*. 'Hour' is the hour of the day when the measurements were taken. The observed data was taken from Beale *et al*. (1996).

most measurement days during the growing season, except the first measurement day, June 1, where the model overpredicted CO_2 uptake (Fig. 3). This can possibly be attributed to the low temperatures preceding this date, which normally occur in the early growing season in United Kingdom (Beale *et al*., 1996). Controlled environment studies have shown that growth at mean daytime temperatures below 12 °C decreases photosynthetic capacity (Beale *et al*., 1996; Farage *et al*., 2006). The effect of low temperatures on leaf photosynthesis through photoinhibition is a critical factor for both future development of models for biomass crops as well as a target for breeding efforts, since the ability to photosynthesize at lower temperatures could increase the length of the growing season and the period of maximum growth rate.

Simulated yields also closely followed observed yields throughout the growing season for all *M.* × *giganteus* studies across a wide range of locations in western Europe (Fig. 4). Not only were final yields predicted well, at most locations, but also growth in terms of shoot biomass accumulation across the growing season. The close agreement between simulated and observed data was observed in studies ranging from Ireland to Greece, suggesting that the model was able to account for the variability in environmental conditions. The largest discrepancy was seen in a study conducted in Catania, Sicily ('Italy 93 and Italy 94', Fig. 4) (Foti *et al*., 1996), where *M.* × *giganteus* showed peak yield much later in the growing season than predicted by the model and than observed at other sites (Foti *et al*., 1996; Cosentino *et al*., 2007). Some reasons for the disagreement can be discarded: (1) genotype differences; all plants were cloned from the same source; (2) temperatures; these were similar to those in Greece where this was not evident (Danalatos *et al*., 2007; Cosentino *et al*., 2007). Severe drought which occurred in Catania, but not in Greece, might be responsible for the delayed development. Indeed, irrigation in the second growing season accelerated *M.* × *giganteus* flowering in Catania (Cosentino *et al*., 2007). This indicates that the model may fail to capture the effects of water stress on the duration of phenological stages and it is an area where future model development will improve accuracy by allowing more flexibility in the response of C allocation in response to environmental factors. In addition, it is expected that this is a major source of genotypic variability since there are notable differences within the *Miscanthus* genus in their response to water stress (Clifton-Brown & Lewandowski, 2000) with *M. sinensis* being a more conservative user of water through a lower leaf area and stomatal conductance than *M.* × *giganteus* and thus better suited for drier environments.

Compilation of all the predicted with their parallel observed biomass samplings for all sites (Fig. 5) suggested that, with current parameterization, shoot (Fig. 5), stem mass (Fig. 6) and leaf area index (Fig. 7) were slightly overpredicted. The tendency toward overprediction can potentially be contributed to several factors: (1) the impact of nutrient deficiencies and weed competition on biomass accumulation were not incorporated in the current model; (2) at some northern locations high light intensities and low temperatures can cause photo-

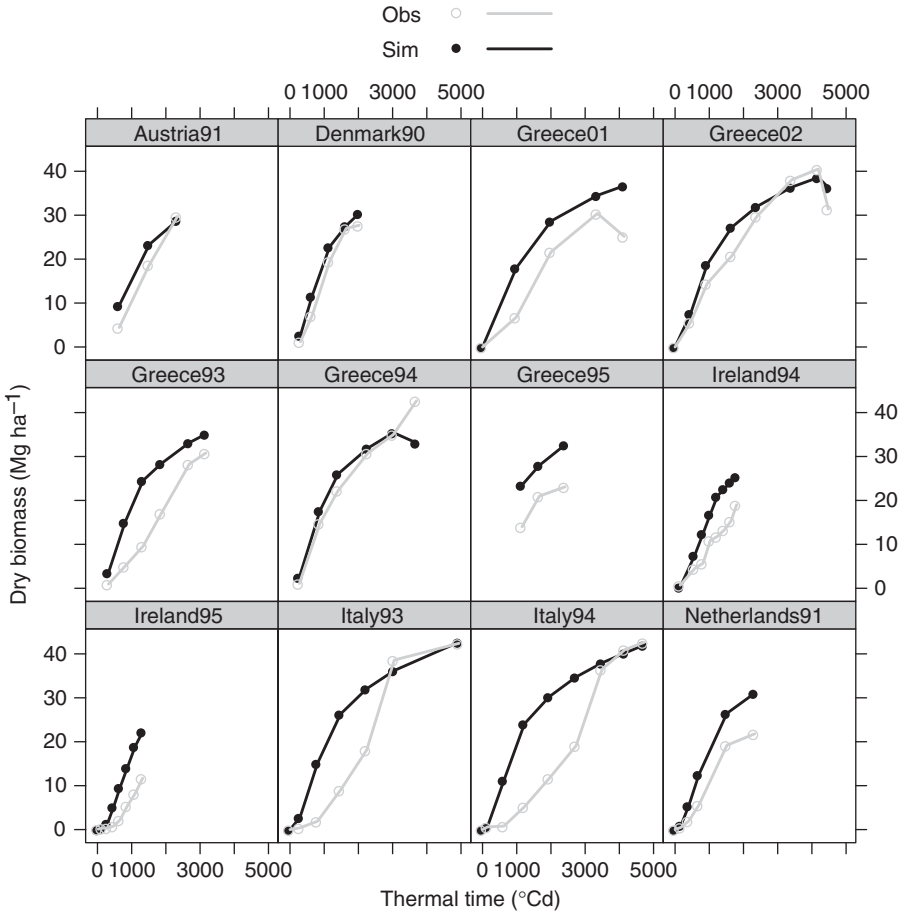

Fig. 4 Observed (open circles, blue) and predicted (closed circles, black) *M.* × *giganteus* above ground dry biomass in multiple year and location experiments in Europe as a function of thermal time. Each panel has first the name of the location where the experiment was conducted followed by the last two digits of the year. Austria91 (Schwarz *et al*., 1994), Denmark90 (Jorgensen, 1996), Greece01, 02 (Danalatos *et al*., 2007), Greece93, 94, 95 (Dalianis *et al*., 1994; Danalatos *et al*., 1996, 1998), Ireland94, 95 (Clifton-Brown *et al*., 2000), Italy93, 94 (Foti *et al*., 1996), Netherlands91 (van der Werf *et al*., 1992).

damage and reduce growth (Long *et al*., 1983); (3) limitations in the model structure and parameterization of the model. As more experiments are conducted on *M.* × *giganteus* and more growth data are available, better parameterization will be possible. In addition, there is also a need for better algorithms for parameter estimation in crop models which will allow to get point estimates as well as a measure of the uncertainty in the parameters of interest (Wallach *et al*., 2001; Miguez, 2008).

Features and limitations of using a semimechanistic crop model

WIMOVAC is characterized by its emphasis on process-based description of physiological processes. This immediately results in a model with more detail and, in general, with greater data requirements for its parameterization for a given crop. This greater data requirement can be seen as a limitation, but it also highlights the need for additional research in basic aspects of *M.* × *giganteus* physiology (Jorgensen & Schwarz, 2000). In this study dry biomass partitioning was parameterized with studies conducted in the United Kingdom, but substantially uncertainty remains regarding the modification of the partitioning coefficients under different environments (locations and/or years). However, the model was able to simulate the dynamics of dry biomass accumulation during the growing season in different environments (Fig. 4) and these dynamics are needed for accurate modeling of nutrient, carbon and water cycles, which are critical for determining the potential for carbon sequestration and the nutrient and water requirements of a biofuel crop such as *M.* × *giganteus*. An important aspect in biomass crops simulations and *M.* × *giganteus* in particular is the trade-off between early and late harvest (Miguez *et al*., 2008) which depends greatly on its end use (Lewandowski & Heinz, 2003). Modelling yield losses due to leaf senescence, nutrient translocation to the rhizomes

and stem and leaf drop remains a challenge since these physiological processes are not well understood, but nevertheless are of great importance in producing accurate estimates of harvestable biomass. In addition, a model which incorporates yield losses should possibly account for severe weather which can greatly reduce harvestable biomass (Lewandowski *et al*., 2003).

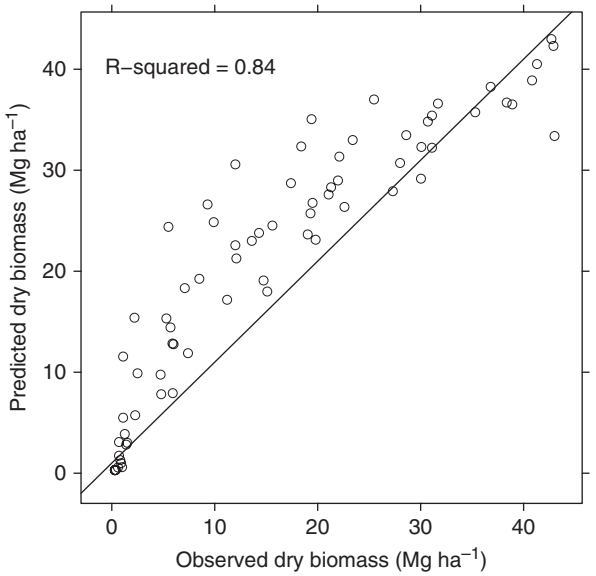

Fig. 5 Observed vs. simulated *M.* × *giganteus* above ground dry biomass in multiple year and location experiments in Europe ($R^2 = 0.84$). The line is the 1 : 1 relationship. Points closer to the line reflect a higher agreement between observed and predicted.

Comparison of WIMOVAC with other models used for M. × giganteus

Other models have been proposed for modeling *M.* × *giganteus* (Clifton-brown *et al*., 2004; Price *et al*., 2004; Hastings *et al*., 2009) and these models have been successful at capturing the potential for growing this crop in different regions. The main difference between WIMOVAC and these models is the emphasis on physiological details, which increases the number of parameters and the amount and quality of data needed to parameterize the model. As a result the quality and the detail of the simulations also increase. For example, in this manuscript we showed how the model was able to capture hourly leaf-level photosynthesis (Fig. 3) which becomes relevant when the objective of the simulation is to predict the effect of future climate scenarios (increase temperature, CO_2 and vapour pressure deficit) on the performance of biomass crops. Currently, WIMOVAC does not model moisture content in the biomass or rhizome and shoot death due to cold temperatures or extended periods of water stress as it has been recently incorporated in MISCANFOR (Hastings *et al*., 2009). A combination of information derived from field studies and process-based description of physiological process incorporated in WIMOVAC is needed in order to improve simulations of growth and productivity of biomass crops such as *M.* × *giganteus*.

Conclusions

In summary, we adapted WIMOVAC for the biomass crop *M.* × *giganteus* and demonstrated that it can closely

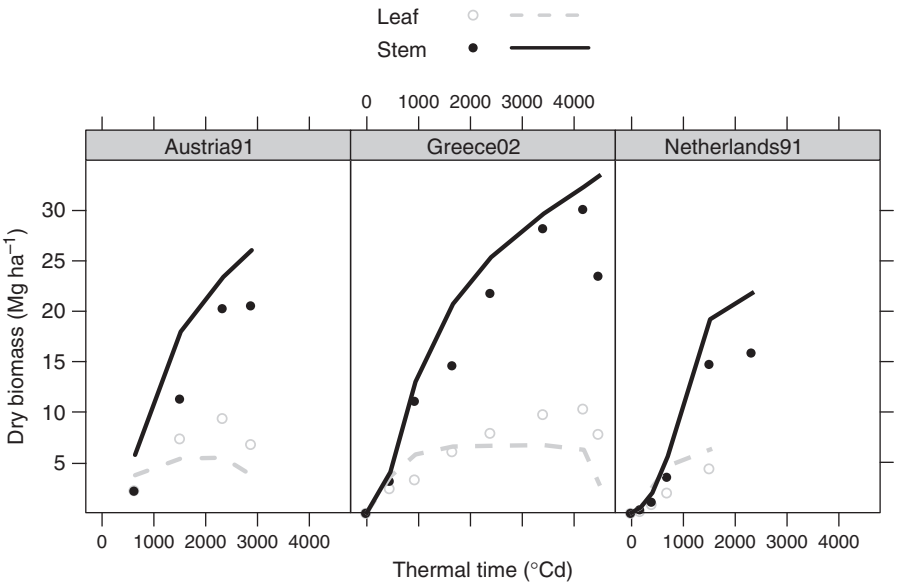

Fig. 6 Observed (circles) and simulated (lines) dry biomass of *M.* × *giganteus* in multiple year and location experiments in Europe. The solid lines are the stem and the dashed lines are the leaf dry biomass. See Fig. 4 for details.

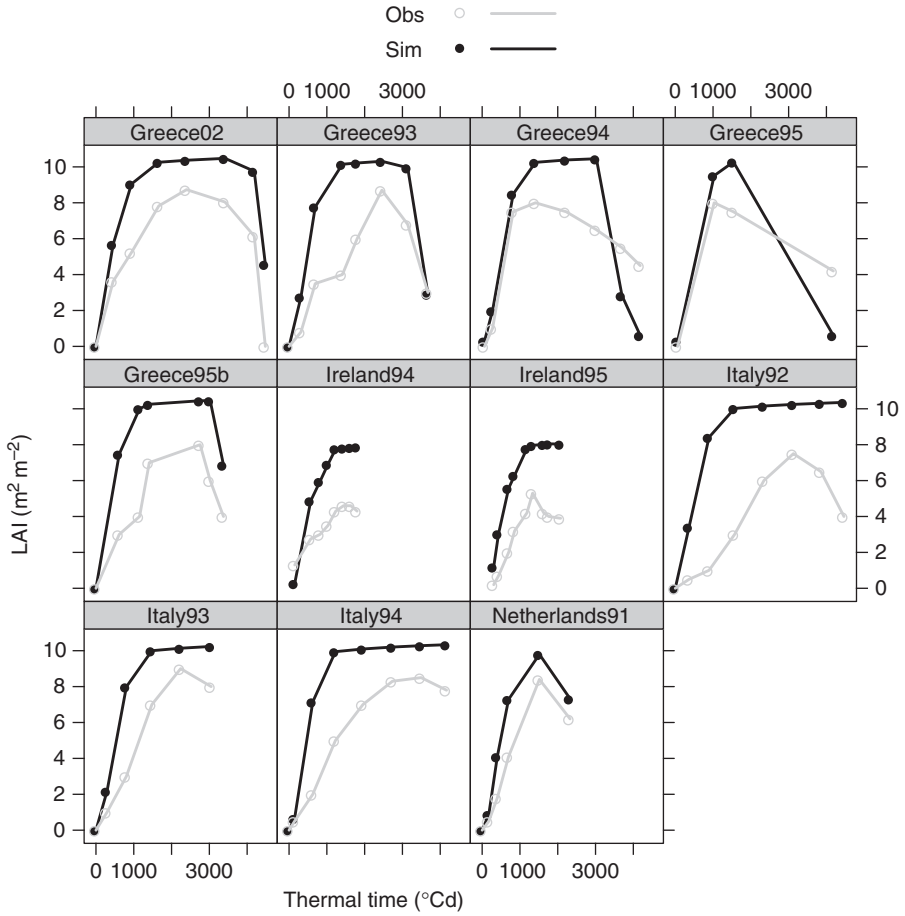

Fig. 7 Observed (open circles, blue) and simulated (closed circles, black) leaf area index (LAI) of *M.* × *giganteus* in multiple year and location experiments in Europe. See Fig. 4 for details.

predict field diurnal CO_2 uptake of *M.* × *giganteus* and biomass accumulation patterns through the growing season at different sites in Europe. The current model and parameterization tended to overpredict leaf area index and biomass accumulation. As a mechanistically rich model, this provides a vehicle for numerical experiments that may allow optimization of field experiments and long-term breeding and selection. For example, would yield benefit from a decreased or increased LAI or from a larger or smaller proportional investment in rhizome mass? At the same time it provides a framework for predicting yields outside the current range of experience in Europe and a means to assess the benefit of addition of physiological traits found in other *M.* × *giganteus* germplasm.

Acknowledgements

We would like to acknowledge Clive Beale and Sotiris Archontoulis for providing data from their publications.

References

Beale CV, Bint DA, Long SP (1996) Leaf photosynthesis in the C4-grass *Miscanthus* × *giganteus*, growing in the cool temperate climate of southern England. *Journal of Experimental Botany*, **47**, 267–273.

Beale CV, Long SP (1995) Can perennial C4 grasses attain high efficiencies of radiant energy conversion in cool climates? *Plant, Cell and Environment*, **18**, 641–650.

Beale CV, Long SP (1997) Seasonal dynamics of nutrient accumulation and partitioning in the perennial C4-grasses *Miscanthus* × *giganteus* and *Spartina cynosuroides*. *Biomass and Bioenergy*, **12**, 419–428.

Campbell GS (1991) Simulation of water uptake by plant roots. In: *Modelling Plant and Soil Systems*, Vol. 31, (eds Hanks J, Ritchie JT), pp. 273–285. Americal Society of Agronomy, Madison.

Cao W, Moss DN (1997) Modelling phasic development in wheat: a conceptual integration of physiological components. *Journal of Agricultural Science*, **129**, 163–172.

Chung S-O, Horton R (1987) Soil heat and water flow with a partial surface mulch. *Water Resources Research*, **23**, 2157–2184.

Clifton-Brown JC, Lewandowski I (2000) Water use efficiency and biomass partitioning of three different miscanthus geno-

types with limited and unlimited water supply. *Annals of Botany*, **86**, 191–200.

Clifton-Brown JC, Long SP, Jorgensen U (2001) Miscanthus productivity. In: *Miscanthus for Energy and Fiber* (eds Jones MB, Walsh M), pp. 46–67. James & James (Science Publishers) Ltd, London.

Clifton-Brown JC, Neilson B, Lewandowski I, Jones MB (2000) The modelled productivity of *Miscanthus × giganteus* (GREEF et DEU) in Ireland. *Industrial Crops and Products*, **12**, 97–109.

Clifton-brown JC, Stampfl PF, Jones MB (2004) Miscanthus biomass production for energy in Europe and its potential contribution to decreasing fossil fuel carbon emissions. *Global Change Biology*, **10**, 509–518.

Collatz GJ, Ribas-Carbo M, Berry JA (1992) Coupled photosynthesis-stomatal conductance model for leaves of C4 plants. *Australian Journal Of Plant Physiology*, **19**, 519–538.

Cosentino SL, Patane C, Sanzone E, Copani V, Foti S (2007) Effects of soil water content and nitrogen supply on the productivity of *Miscanthus × giganteus* Greef et Deu. in a Mediterranean environment. *Industrial Crops and Products*, **25**, 75–88.

Dalianis CD, Sooter CA, Christou MG (1994) Growth, biomass productivity, and energy potential of giant reed (*Arnudo donax*) and elephant grass (*Miscanthus sinensis giganteus*) In: *Proceedings of the Eighth European Biomass Conference*, Vienna, Pergamon, UK, pp. 575–582.

Danalatos NG, Archontoulis SV, Mitsios I (2007) Potential growth and biomass productivity of *Miscanthus × giganteus* as affected by plant density and N-fertilization in central Greece. *Biomass and Bioenergy*, **31**, 145–152.

Danalatos NG, Dalianis C, Kyristis S (1996) Growth and biomass productivity of *Miscanthus sinensis* ''Giganteus'' under optimum cultural management in north-eastern Greece 548–553.

Danalatos NG, Dalianis C, Kyristis S (1998) Influence of fertilisation and irrigation on the growth and biomass productivity of *Miscanthus sinensis × giganteus* under Greek conditions. In: *Sustainable Agriculture for Food Energy and Industry*, **Vol. 1** (ed. Anonymous) pp. 319–323. James & James, Science Publishers, Braunschweig, Germany.

Demetriades-Shah TH, Fuchs M, Kanemasu ET, Flitcroft I (1992) A note of caution concerning the relationship between cumulated intercepted solar radiation and crop growth. *Agricultural and Forest Meteorology*, **58**, 193–207.

Farage PK, Blowers D, Long SP, Baker NR (2006) Low growth temperatures modify the efficiency of light use by photosystem II for CO_2 assimilation in leaves of two chilling-tolerant C4 species, *Cyperus longus* L. and *Miscanthus × giganteus*. *Plant, Cell and Environment*, **29**, 720–728.

Farrell AE, Plevin RJ, Turner BT, Jones AD, O'Hare M, Kammen DM (2006) Ethanol can contribute to energy and environmental goals. *Science*, **311**, 506–508.

Forseth I, Norman J (1991) Photosynthesis and productivity research in a changing environment. In: *Modeling of Solar Irradiance, Leaf Energy Budget, and Canopy Photosynthesis*, pp. 207–219. Chapman & Hall, London.

Foti S, Cosentino SL, Patane C, Guarnaccia P (1996) Growth and yield for C4 species for biomass production in the Mediterranean environment. In *'Biomass for Energy and the Environment'. Proceedings of the 9th European Bioenergy Conference*, pp. 616–621. Pergamon/Elseveier, Copenhagen, Denmark.

Hastings A, Clifton-Brown J, Wattenbach M, Mitchell C, Smith P (2009) The development of MISCANFOR, a new *Miscanthus* crop growth model: towards more robust yield predictions under different climatic and soil conditions. *GCB Bioenergy*, **1**, 154–170.

Heaton E, Voigt T, Long SP (2004) A quantitative review comparing the yields of two candidate C4 perennial biomass crops in relation to nitrogen, temperature and water. *Biomass and Bioenergy*, **27**, 21–30.

Heaton EA, Dohleman FG, Long SP (2008) Meeting US biofuel goals with less land: the potential of *Miscanthus*. *Global Change Biology*, **14**, 2000–2014.

Hodkinson T, Renvoize S (2001) Nomenclature of *Miscanthus × giganteus* (Poaceae). *Kew Bulletin*, **56**, 759–760.

Humphries S, Long SP (1995) WIMOVAC – a software package for modeling the dynamics of the plant leaf and canopy photosynthesis. *Computer Applications in the Bioscience*, **11**, 361–371.

Jorgensen U (1996) *Miscanthus* yields in Denmark. In: *Biomass for Energy and the Environment. Proceedings of the 9th European Bioenergy Conference*, pp. 48–53. Pergamon/Elsevier, Copenhagen, Denmark.

Jorgensen U, Schwarz KU (2000) Why do basic research? A lesson from commercial exploitation of *Miscanthus*. *New Phytologist*, **148**, 190–193.

Koonin SE (2006) Getting serious about biofuels. *Science*, **311**, 435.

Lewandowski I, Clifton-Brown J, Scurlock JMO, Huisman W (2000) *Miscanthus*: European experience with a novel energy crop. *Biomass and Bioenergy*, **19**, 209–227.

Lewandowski I, Clifton-Brown JC, Andersson B *et al*. (2003) Environment and harvest time affects the combustion qualities of *Miscanthus* genotypes. *Agronomy Journal*, **95**, 1274–1280.

Lewandowski I, Heinz A (2003) Delayed harvest of *Miscanthus*-influences on biomass quantity and quality and environmental impacts of energy production. *European Journal of Agronomy*, **19**, 45–63.

Long SP, East TM, Baker NR (1983) Chilling damage to photosynthesis in young *Zea mays*: I. Effects of light and temperature variation on photosynthetic CO_2 assimilation. *Journal of Experimental Botany*, **34**, 177–188.

Loomis RS, Amthor JS (1999) Yield potential, plant assimilatory capacity, and metabolic efficiencies. *Crop Science*, **39**, 1584–1596.

Miguez FE (2008) Parameter Esimtation in Biomass Crop Models. In: *Ecological Society of America*. Milwaukee, WI.

Miguez FE, Villamil MB, Long SP, Bollero GA (2008) Meta-analysis of the effects of management factors on *Miscanthus × giganteus* growth and biomass production. *Agricultural and Forest Meteorology*, **148**, 1280–1292.

Monteith JL (1973) *Principles of Environmental Physics*. Edward Arnold, London.

Naidu SL, Moose SP, Al-Shoaibi AK, Raines CA, Long SP (2003) Cold tolerance of C4 photosynthesis in *Miscanthus × giganteus*: adaptation in amounts and sequence of C4 photosynthetic enzymes. *Plant Physiology*, **132**, 1688–1697.

Norman JM (1980) Predicting photosynthesis for ecosystem models. In: *Interfacing leaf and canopy light interception models* (eds Hesketh JDJ, Jones JW), pp. 49–67. CRC Press, Boca Raton, FL.

Penman HL (1948) Natural evaporation from open water, bare soil and grass. *Proceedings of the Royal Society of London: Series B*, **193**, 120–145.

Penning de Vries FWT (1972) Respiration and growth. In: *Crop processes in controlled, environments* (eds Rees AR, Cockshull KE, Hand DW, Hurd RJ), pp. 327–347. Academic Press, London.

Price L, Bullard M, Lyons H, Anthony S, Nixon P (2004) Identifying the yield potential of *Miscanthus* × *giganteus*: an assessment of the spatial and temporal variability of *M.* × *giganteus* biomass productivity across England and Wales. *Biomass and Bioenergy*, **26**, 3–13.

Ragauskas AJ, Williams CK, Davison BH *et al*. (2006) The path forward for biofuels and biomaterials. *Science*, **311**, 484–489.

Reddy SJ (1995) Over-emphasis on energy terms in crop yield models. *Agricultural and Forest Meteorology*, **77**, 113–120.

Schwarz H, Liebhard P, Ehrendorfer K, Ruckenbauer P (1994) The effect of fertilization on yield and quality of *Miscanthus sinensis* 'Giganteus'. *Industrial Crops and Products*, **2**, 153–159.

Spain JD, Keen RD (1992) Temperature and biological activity. In: *Computer Simulation in Biology: A Basic Introduction* (eds Keen RE, Spain JD), pp. 183–200. John Wiley & Sons Inc., New York.

U.S.DOE (2006) Breaking the biological barriers to cellulosic ethanol: a joint research agenda, DOE/SC-0095, U.S. Department of Energy Office of Science and Office of Energy and Renewable Energy (www.doegenomestolife.org/biofuels).

van der Werf HMG, Meijer WJM, Mathijssen EWJM, Darwinkel A (1992) Potential dry matter production of *Miscanthus sinensis* in The Netherlands. *Industrial Crops and Products*, **1**, 203–210.

Wallach D, Goffinet B, Bergez J-E, Debaeke P, Leenhardt D, Aubertot J-N (2001) Parameter estimation for crop models: a new approach and application to a corn model. *Agron Journal*, **93**, 757–766.

World Meteorological Organization. (2007). Available at http://www.wmo.ch/pages/index_en.html [Accessed December 2007]

Appendix A The key equations in WIMOVAC-related to simulating *M.* × *giganteus*

$$\delta = -23.5\mathrm{Cos}\left(\frac{360(D_\mathrm{j}+10)}{365}\right) \tag{A1}$$

$$\cos(\theta) = \sin(\Omega)\sin(\delta) + \cos(\Omega)\cos(\delta)\cos(15(t - t_\mathrm{sn})) \tag{A2}$$

$$I_\mathrm{dir} = I_\mathrm{s}\alpha^{((P/P_\mathrm{o})/\cos(\theta))} \tag{A3}$$

$$I_\mathrm{diff} = 0.5I_\mathrm{s}(1 - \alpha^{(P/P_\mathrm{o})/\cos(\theta)})\cos(\theta) \tag{A4}$$

$$\cos\left(\frac{15t_\mathrm{len}}{2}\right) = -\tan(\lambda)\tan(\delta) \tag{A5}$$

$$\mathrm{Mean} = T_1 + T_2\sin\left(2\pi\frac{D_\mathrm{j} - D_\mathrm{start}}{365}\right) \tag{A6}$$

$$\mathrm{Range} = T_3 + (T_4 - T_3)\sin\left(2\pi\frac{D_\mathrm{j} - D_\mathrm{start}}{365}\right) \tag{A7}$$

$$\mathrm{Excursion} = \sin\left(2\pi\frac{h_\mathrm{r} - 10}{24}\right) \tag{A8}$$

$$T_\mathrm{air} = \mathrm{Mean} + \mathrm{Range} \times \mathrm{Excursion} \tag{A9}$$

$$V_\mathrm{cmax} = V_\mathrm{cmaxo}\mathrm{K_t}(E_\mathrm{vcmax}) \tag{A10}$$

$$R_\mathrm{d} = R_\mathrm{o}\mathrm{K_t}(E_\mathrm{Rd}) \tag{A11}$$

$$M = \min\frac{(V_\mathrm{cmax} + \alpha_\mathrm{slope}I_\mathrm{abs}) \pm \sqrt{(V_\mathrm{cmax} + \alpha_\mathrm{slope}I_\mathrm{abs})^2 - 4(V_\mathrm{cmax}\alpha_\mathrm{slope}I_\mathrm{abs})\theta_\mathrm{curve}}}{2\theta_\mathrm{curve}} \tag{A12}$$

$$A_\mathrm{gross} = \min\frac{\left(M + k_\mathrm{t}\left(\frac{c_\mathrm{i}}{P}\right)\right) \pm \sqrt{\left(M + k_\mathrm{t}\left(\frac{c_\mathrm{i}}{P}\right)\right)^2 - \left(4Mk_\mathrm{t}\left(\frac{c_\mathrm{i}}{P}\right)\beta\right)}}{2\beta} \tag{A13}$$

$$A_\mathrm{n} = A_\mathrm{gross} - R_\mathrm{d} \tag{A14}$$

$$h_\mathrm{s} = \frac{e_l - \mathrm{VPD}}{e_l}100 \tag{A15}$$

$$g_\mathrm{s} = g_0 + g_1A_\mathrm{gross}\left(\frac{h_\mathrm{s}}{C_\mathrm{a}}\right) \tag{A16}$$

$$g_\mathrm{wmod} = \left(\frac{(\Psi_\mathrm{l} - \Psi_\mathrm{t})}{1000}\right)g_\mathrm{ws} \tag{A17}$$

$$g_1 = g_1(1 - g_\mathrm{wmod}) \tag{A18}$$

$$k = \frac{\sqrt{\chi^2 + \tan^2(\theta)}\cos(\theta)}{\chi + 1.744[\chi + 1.183]^{-0.733}} \quad \text{(A19)}$$

$$F_{\text{sun}} = \frac{[1\text{e}^{(-kF_{\text{canopy}}/\cos(\theta))}]\cos(\theta)}{k} \quad \text{(A20)}$$

$$F_{\text{shade}} = F_{\text{canopy}} - F_{\text{sun}} \quad \text{(A21)}$$

$$F_{\text{canopy}} = F_{\text{sun}} + F_{\text{shade}} \quad \text{(A22)}$$

$$I_{\text{sun}} = I_{\text{dir}}k/\cos(\theta)) + I_{\text{shade}} \quad \text{(A23)}$$

$$I_{\text{shade}} = I_{\text{diff}}e^{(-0.5F^{0.7}_{\text{canopy}})} + I_{\text{scat}} \quad \text{(A24)}$$

$$I_{\text{scat}} = 0.07I_{\text{dir}}(1.1 - 0.1f)\text{e}^{-(\text{Cos}(\theta))} \quad \text{(A25)}$$

$$I_{\text{total}} = I_{\text{dir}} + I_{\text{dif}} \quad \text{(A26)}$$

$$A_{\text{c}} = (A_{\text{c,sun}}F_{\text{sun}}) + (A_{\text{c,shade}}F_{\text{shade}}) \quad \text{(A27)}$$

$$\text{F}_{\text{sun}} = \sum_{\text{layerN}}^{\text{layer1}} \text{l}_{\text{sun}}; \quad \text{l}_{\text{sun}} = \frac{1-\text{e}^{(-\text{k}F_{\text{sun}})}}{\text{k}} \quad \text{(A28)}$$

$$F_{\text{shade}} = \sum_{\text{layerN}}^{\text{layer1}} \ell_{\text{shade}}; \quad \ell_{\text{shade}} = F_{\text{sum}} - \ell_{\text{sun}} \quad \text{(A29)}$$

$$F_{\text{canopy}} = F_{\text{sun}} + F_{\text{shade}} \quad \text{(A30)}$$

$$I_{\text{d}} = I_{\text{diff}}\exp^{(-kF_{\text{sum}})} \quad \text{(A31)}$$

$$I_{\ell,\text{d}} = kI_{\text{d}} \quad \text{(A32)}$$

$$I_{\ell,\text{s}} = kI_{\text{dir}} + I_{\ell,\text{d}} \quad \text{(A33)}$$

$$A_{\text{c}} = \sum_{\text{layerN}}^{\text{layer1}} (A_{\text{c,sun}}F_{\text{sun}}) + (A_{\text{c,shade}}F_{\text{shade}}) \quad \text{(A34)}$$

$$A_{\text{c,tot}} = \int_{D_{\text{j}}=365}^{D_{\text{j}}=1} \int_{\text{hr}=24}^{\text{hr}=0} A_{\text{c}} \quad \text{(A35)}$$

$$g_{\text{c}} = \sum_{\text{layerN}}^{\text{layer1}} (g_{\text{s,sun}}l_{\text{sun}}) + (g_{\text{s,shade}}l_{\text{shade}}) \quad \text{(A36)}$$

$$g_{\text{c,tot}} = \int_{D_{\text{j}}=365}^{D_{\text{j}}=1} \int_{\text{hr}=24}^{\text{hr}=0} g_{\text{c}} \quad \text{(A37)}$$

$$J_{\text{a}} = 2I_{\text{abs}}\left(\frac{1-r-\tau}{1-\tau}\right)\ell \quad \text{(A38)}$$

$$L_{\text{b}} = (2.126 \cdot 10^{-5} + 1.48 \cdot 10^{-7}T_{\text{air}})/0.004\sqrt{L_{\text{w}}/u_{\text{layer}}} \quad \text{(A39)}$$

$$u_{\text{a}} = \frac{u0.41}{\log((u-d)/z_{\text{o}})} \quad \text{(A40)}$$

$$g_{\text{a}} = \frac{(u_{\text{a}}^2/u_{\text{layer}})L_{\text{b}}}{(u_{\text{a}}^2/u_{\text{layer}}) + L_{\text{b}}} \quad \text{(A41)}$$

$$\rho'_v = 610.78\text{e}^{\left(17.269\frac{T_{\text{a}}}{T_{\text{a}}+237.3}\right)} \quad \text{(A42)}$$

$$\Delta\rho_{\text{va}} = \rho'_v\left(1 - \frac{h_{\text{s}}}{100}\right) \quad \text{(A43)}$$

$$\gamma = \frac{\rho c_{\text{P}}}{\lambda} \quad \text{(A44)}$$

$$s = 18(2501 - 2.373T_{\text{a}})\left(\frac{\rho'_v}{8.314(T_{\text{a}}+273)^2}\right) \quad \text{(A45)}$$

$$R_{\text{lc}} = 45.6710^{-8}(273 + T_{\text{air}})^3\Delta T \quad \text{(A46)}$$

$$\Phi_{\text{N}} = J_{\text{a}} - R_{\text{lc}} \quad \text{(A47)}$$

$$\Delta T = T_{\text{leaf}} - T_{\text{air}} = \frac{\Phi_{\text{n}}\left(\frac{1}{g_{\text{a}}} + \frac{1}{g_{\text{c}}}\right)}{\lambda\left[s + \gamma\left(1 + \frac{g_{\text{a}}}{g_{\text{c}}}\right)\right]} - \frac{\lambda\Delta\rho_{\text{va}}}{\left[s + \gamma\left(1 + \frac{g_{\text{a}}}{g_{\text{c}}}\right)\right]} \quad \text{(A48)}$$

$$E = \frac{s\Phi_{\text{N}} + \lambda\gamma g_{\text{a}}\Delta\rho_{\text{va}}}{\lambda[s + \gamma(1 + g_{\text{a}}/g_{\text{c}})]} \quad \text{(A49)}$$

$$\mathbf{E}_{\text{c}} = \sum_{\text{layer}N}^{\text{layer1}} (\mathbf{E}_{\text{sun}}l_{\text{sun}}) + (\mathbf{E}_{\text{shade}}l_{\text{shade}}) \quad \text{(A50)}$$

$$\mathbf{E}_{\text{tot}} = \int_{D_{\text{j}}=365}^{D_{\text{j}}=1} \int_{\text{hr}=24}^{\text{hr}=0} \mathbf{E}_{\text{c}} \quad \text{(A51)}$$

$$A_{\text{stroot}} = abs(\omega_{\text{stroot}}k_{\text{stroot}}); \quad k_{\text{stroot}} < 0 \quad \text{(A52)}$$

$$A_{\text{total}} = A_{\text{c}} + A_{\text{seed}} + A_{\text{stroot}} \quad \text{(A53)}$$

$$\omega_{\text{leaf}} = \omega_{\text{leaf}} + (A_{\text{total}}k_{\text{leaf}}) \quad \text{(A54)}$$

$$\omega_{\text{stem}} = \omega_{\text{stem}} + (A_{\text{total}} k_{\text{stem}}) \tag{A55}$$

$$\omega_{\text{sroot}} = \omega_{\text{sroot}} + (A_{\text{total}} k_{\text{sroot}}) \tag{A56}$$

$$\omega_{\text{stroot}} = \omega_{\text{stroot}} + (A_{\text{total}} k_{\text{stroot}}) \tag{A57}$$

$$\omega_{\text{froot}} = \omega_{\text{leaf}} + (A_{\text{total}} k_{\text{froot}}) \tag{A58}$$

$$\begin{gathered} \boldsymbol{\Psi}_{\text{adl}} < \boldsymbol{\Psi}_{\text{pt}}; \\ k_{\text{leaf}} = k_{\text{leaf}} k_{\text{mod}} \\ k_{\text{stem}} = k_{\text{stem}} k_{\text{mod}} \\ k_{\text{stroot}} = k_{\text{stroot}} k_{\text{mod}} \end{gathered} \tag{A59}$$

$$k_{\text{mod}} = (\boldsymbol{\Psi}_{\text{adl}} - \boldsymbol{\Psi}_{\text{pt}})\boldsymbol{\Psi}_{\text{g}} \quad 0 \le k_{\text{mod}} \le 1 \tag{A60}$$

$$\Delta F_{\text{canopy}} = \frac{\omega_{\text{leaf}}}{Sp_{\text{leaf}}} \tag{A61}$$

$$\Delta L_{\text{stem}} = \frac{\omega_{\text{stem}}}{Sp_{\text{stem}}} \tag{A62}$$

$$\Delta L_{\text{sroot}} = \frac{\omega_{\text{root}}}{Sp_{\text{sroot}}} \tag{A63}$$

$$\Delta L_{\text{stroot}} = \frac{\omega_{\text{stroot}}}{Sp_{\text{stroot}}} \tag{A64}$$

$$\begin{aligned} R_{\text{total}} = (aA_{\text{gross}}) + (b_{\text{leaf}}\omega_{\text{leaf}}) + (b_{\text{stem}}\omega_{\text{stem}}) \\ + (b_{\text{root}}\omega_{\text{root}}) \end{aligned} \tag{A65}$$

$$E_{\text{soil}} = \sum \frac{(\psi_{\text{si}} - gz_{\text{i}} - \psi_{\text{x}})}{R_{\text{si}} + R_{\text{ri}}} \tag{A66}$$

$$R_{\text{ri}} = R_{\text{r}} \frac{(\sum L_{\text{i}})}{L_{\text{i}}} \tag{A67}$$

$$\psi_{\text{x}} = \sum \frac{(\psi_{\text{si}} - q_{\text{w}} z_{\text{i}})}{R_{\text{si}} + R_{\text{ri}}} \Big/ \sum \frac{1}{R_{\text{si}} + R_{\text{ri}}} \tag{A68}$$

$$\psi_{\text{L}} = \psi_{\text{x}} - ER_{\text{L}} \tag{A69}$$

$$E_{\text{d}} = \begin{cases} E_{\text{p},} & \theta^* \ge \theta_1 \\ E_{\text{p}}\left(\frac{\theta - \theta_2}{\theta_1 - \theta_2}\right), & \theta_2 < \theta^* < \theta_1 \\ 0, & \theta^* \le \theta_2 \end{cases} \tag{A70}$$

$$\theta_{\text{i+1}} = \theta_{\text{i}} - \frac{E_{\text{i}}(\theta_{\text{i}})}{\rho_{\text{w}} d_{\text{s}}} \tag{A71}$$

$$g_{\text{a,soil}} = \frac{2.126 \cdot 10^{-5} + 1.48 \cdot 10^{-7} T_{\text{soil}}}{0.004\sqrt{\frac{S_{\text{size}}}{u_{\text{soil}}}}} \tag{A72}$$

$$R_{\text{lc,soil}} = 45.67 \cdot 10^{-8}(273 + T_{\text{soil}})^3 \Delta T \tag{A73}$$

$$J_{\text{a}}, \text{soil} = 2I_{\text{soil}}\left(\frac{1 - S_{\text{r}} - S_{\tau}}{1 - S_{\tau}}\right) \tag{A74}$$

$$\Phi_{\text{N,soil}} = J_{\text{a,soil}} - R_{\text{lc,soil}} \tag{A75}$$

$$E = \frac{s\Phi_{\text{N,soil}} + \lambda\gamma g_{\text{a,soil}} \Delta\rho_{\text{va}}}{\lambda[s + \gamma]} \tag{A76}$$

$$HS_{\text{soil}} = HO_{\text{soil}} \exp\left[\frac{h_{\text{soil}}}{46.97(T_{\text{s}} + 273.16)}\right] \tag{A77}$$

$$HO_{\text{soil}} = 1.323 \exp\left[\frac{17.27T_{\text{s}}}{273.3 + T_{\text{s}}}\right] \Big/ T_{\text{s}} + 273.16 \tag{A78}$$

$$G_{\text{soil}} = -\lambda_{\text{soil}} \frac{\delta T}{\delta z} \tag{A79}$$

$$G_{\text{soil}} = -\lambda_{\text{soil}}\left[\frac{T_2 - T_{\text{s}}}{\Delta z}\right] + (T_{\text{s}} - T_1)C\frac{\Delta z}{(2\Delta t)} \tag{A80}$$

Appendix B

Table B1 Definition of Abbreviations

Term	Units	Definition	Value/reference
A_{gross}	$\mu mol\,mol^{-1}$	Gross rate of CO_2 uptake per unit leaf area	–
A_{net}	$\mu mol\,mol^{-1}$	Net rate of CO_2 uptake per unit leaf area	–
A_c	$\mu mol\,mol^{-1}$	Net canopy rate of CO_2 uptake per unit ground area	–
$A_{c,tot}$	$g\,m^{-2}\,yr^{-1}$	Ac integrated over the course of a year	–
$A_{c,sun}$	$mol\,mol^{-1}$	Net rate of CO_2 uptake per unit area sunlit leaves	–
$A_{c,shade}$	$mol\,m^{-2}\,s^{-1}$	Net rate of CO_2 uptake per unit area shaded leaves	–
A	$\mu mol\,mol^{-1}$	Predicted rate of CO_2 uptake	–
c_a	$\mu mol\,mol^{-1}$	Atmospheric CO_2 concentration	378 (Collatz *et al*., 1992)
A	Dimensionless	Coefficient for growth respiration	0.2 (Penning de Vries, 1972)
c_i	$\mu mol\,mol^{-1}$	Intercellular concentration of CO_2 in air corrected for solubility relative to 25 °C	–
b_{leaf}	Dimensionless	Coefficient for maintenance respiration for leaf	0.03 (Penning de Vries, 1972)
b_{stem}	Dimensionless	Coefficient for maintenance respiration for stem	0.015 (Penning de Vries, 1972)
b_{root}	Dimensionless	Coefficient for maintenance respiration for root	0.01 (Penning de Vries, 1972)
c_p	$J\,kg^{-1}\,K^{-1}$	Specific heat capacity of dry air	1010
D_j	d	day of year	–
d	Dimensionless	Zero plane displacement	0.77
E	$J\,mol^{-1}$	Activation energy	$R_d = 66405$ $V_{cmax} = 6800$
E_l	$mmol\,m^{-2}\,s^{-1}$	Evapo/transpiration rate at sunlit/shaded leaves in a canopy layer	–
E_c	$mmol\,m^{-2}\,s^{-1}$	Instantaneous canopy evapo/transpiration rate	–
E_{tot}	$mmol\,m^{-2}\,yr^{-1}$	E_c integrated over the course of a year	–
e_L	kPa	Saturated water VPD in the leaf	–
F_{canopy}	$m^2\,m^{-2}$	Canopy leaf area index	–
F_{shade}	$m^2\,m^{-2}$	Canopy shaded leaf area index	–
F_{sun}	$m^2\,m^{-2}$	Canopy sunlit leaf area index	–
F_{sum}	$m^2\,m^{-2}$	Summed leaf area index from top of canopy to layer considered in calculation	–
g_a	$mmol\,m^{-2}\,s^{-1}$	Leaf boundary layer conductance	–
g_s	$mmol\,m^{-2}\,s^{-1}$	Leaf stomatal conductance	–
g_c	$mmol\,m^{-2}\,s^{-1}$	Canopy conductance of CO_2	–
G_0	Dimensionless	Stomatal slope factor	3 (Collatz *et al*., 1992)
G_1	Dimensionless	Stomatal intercept factor	0.08 (Collatz *et al*., 1992)
$g_{s,sun}$	$mmol\,m^{-2}\,s^{-1}$	The sum of stomatal conductance of sunlit leaves	–
$g_{s,shade}$	$mmol\,m^{-2}\,s^{-1}$	The sum of stomatal conductance of shaded leaves	–
h_r	h	Hour of day	–
h_s	%	Relative humidity	–
h_{canopy}	m	Height of canopy	–
h_{ms}	m	Wind speed measurement height	2
h_{layer}	m	Height of canopy layer above ground	–
I	$\mu mol\,m^{-2}\,s^{-1}$	Photon flux	–
I_{abs}	$\mu mol\,m^{-2}\,s^{-1}$	Photon flux absorbed by either sunlit or shaded leaves within a canopy layer	–
I_{dir}	$\mu mol\,m^{-2}\,s^{-1}$	Photon flux in direct solar beam	–
I_{diff}	$\mu mol\,m^{-2}\,s^{-1}$	Photon flux in diffuse radiation	–
I_{total}	$\mu mol\,m^{-2}\,s^{-1}$	Total photon flux incident on canopy	–
I_s	$\mu mol\,m^{-2}\,s^{-1}$	Solar constant, photon flux in a plane perpendicular to the solar beam above the atmosphere	2600
I_{short}	$\mu mol\,m^{-2}\,s^{-1}$	Short wave radiation component of incident light	–
I_{soil}	$\mu mol\,m^{-2}\,s^{-1}$	Solar radiation incident upon soil surface	–
I_{sun}	$\mu mol\,m^{-2}\,s^{-1}$	Mean I for leaves which receive direct solar radiation, i.e. are sunlit	–

Continued

Table B1. (*Contd.*)

Term	Units	Definition	Value/reference
I_{shade}	$\mu mol\,m^{-2}\,s^{-1}$	Mean I for leaves shaded from direct solar radiation	–
I_{scat}	$\mu mol\,m^{-2}\,s^{-1}$	Direct beam radiation scattered by surfaces within the canopy	–
J_a	$\mu mol\,m^{-2}\,s^{-1}$	Total solar radiation absorbed by either sunlit or shaded leaves within a canopy layer	–
K	Dimensionless	Foliar absorption coefficient	–
k_{slope}	Dimensionless	Initial slope of photosynthetic light response	0.04 (Collatz *et al*., 1992)
k_{leaf}	Dimensionless	Partitioning coefficient for leaf	–
k_{stem}	Dimensionless	Partitioning coefficient for stem	–
k_{sroot}	Dimensionless	Partitioning coefficient for storage root	–
k_{froot}	Dimensionless	Partitioning coefficient for fine root	–
k_{stroot}	Dimensionless	Partitioning coefficient for structural root	–
ω_{leaf}	Gram	Leaf biomass	–
ω_{stem}	Gram	Stem biomass	–
ω_{sroot}	Gram	Biomass of storage root	–
ω_{froot}	Gram	Biomass of fine root	–
ω_{stroot}	Gram	Biomass of structural root	–
Sp_{leaf}	$g\,m^{-2}$	Specific leaf area	65
Sp_{stem}	$g\,m^{-1}$	Specific stem elongation factor	60
Sp_{froot}	$g\,m^{-1}$	Specific fine root elongation factor	10
Sp_{stroot}	$g\,m^{-1}$	Specific structural root elongation factor	60
L_w	m	Leaf width in the direction of the wind	0.04
P_s	kPa	Leaf surface partial pressure of CO_2	–
v		Saturated water vapor concentration	–
Q_{10}	Dimensionless	Is the proportional rise in a parameter for a 10°C increase in temperature	2
R	Dimensionless	Leaf reflection coefficient for total solar radiation	0.2
R	$J\,k^{-1}\,mol^{-1}$	Real gas constant	8.314
R_d	$mol\,m^{-2}\,s^{-1}$	Dark respiration at a given temperature	–
R_{lc}	$mol\,m^{-2}\,s^{-1}$	Longwave radiation	–
S	$kPa\,K^{-1}$	Slope of saturated water vapor pressure change with respect to temperature (look up table)	–
s_p	Dimensionless	Spectral imbalance	–
S_{size}	m	Average size of soil particles	0.04
S_r	Dimensionless	Soil reflectance	0.2
S_t	Dimensionless	Soil transmission	0.01
τ	Dimensionless	Leaf transmittance coefficient	
T	h	Time of day	–
t_{sn}	h	Time of solar noon	12
T_{leaf}	°C	Leaf temperature	–
T_{air}	°C	Ambient air temperature	–
T_{soil}	°C	Soil surface temperature	–
T_1	°C	Annual mean air temperature	–
T_2	°C	Annual range in air temperature	–
T_3	°C	Average daily range in air temperature	–
T_4	°C	Maximum daily range in air temperature	–
U	$m\,s^{-1}$	Measured wind speed at known height (2m)	2
u_{layer}	$m\,s^{-1}$	Wind speed in a given canopy layer	–
u_{soil}	$m\,s^{-1}$	Wind speed at soil surface	–
V_{cmax}	$\mu mol\,m^{-2}\,s^{-1}$	Maximum rubP saturated rate of carboxylation	39 (Collatz *et al*., 1992)
VPD	kPa	Leaf-air water vapor pressure deficit	–
z_o	m	Roughness length	0.234
×	Dimensionless	The ratio of horizontal:vertical projected area of leaves in the canopy segment	1

Continued

Table B1. (*Contd.*)

Term	Units	Definition	Value/reference
α	Dimensionless	Atmospheric transmittance	0.85
k_t	$mol\,m^{-1}$	Initial slope of photosynthetic CO_2 response	0.7 (Collatz *et al.*, 1992)
θ_{curve}	Dimensionless	Curvature parameter	0.83 (Collatz *et al.*, 1992)
δ	deg.	Solar declination	–
Ω	deg.	Latitude	–
Θ	deg.	Solar zenith angle	–
λ	MJ/Kg	Latent heat of vapourisation (look up table)	–
γ	$Pa\,K^{-1}$	psychrometer constant (look up table)	–
α_{slope}	$mol\,mol^{-1}$	The quantum yield of CO_2 uptake determined by the initial slope of the response of A vs. I_{abs}	0.04 (Collatz *et al.*, 1992)
β		C4 curvature parameter	0.93 (Collatz *et al.*, 1992)
Kt		C4 slope factor	–
ψ_l	MPa	Leaf water potential	–
ψ_t	MPa	Threshold leaf water potential for decreasing gs	–
Φ_N	$W\,m^{-2}$	Net radiation	–
ψ_{adl}	MPa	Average daily plant water potential	–
ψ_{pt}	MPa	Threshold water potential	–
Z	m	Thickness of a soil layer	–
ψ_x	MPa	Xylem water potential	–
ψ_{si}	MPa	Soil water potential of the ith layer	–
q_w	$Kg\,s^{-1}$	Flux of water	–
R_{si}	$m^3\,kg^{-1}\,s^{-1}$	Soil resistance of the ith zone	–
R_{ri}	$m^3\,kg^{-1}\,s^{-1}$	root resistance of the ith zone	–
L_i	$cm\,cm^{-3}$	Root density of ith zone	–
g	$m\,s^{-2}$	Gravitional constant	9.8
R_L	$m^3\,kg^{-1}\,s^{-1}$	Leaf resistance	–
E_d	$g\,m^{-2}\,s^{-1}$	Potential soil evaporation	–
E_p	$g\,m^{-2}\,s^{-1}$	Actual soil evaporation	–
θ^*	$kg\,m^{-3}$	Actual volumetric water content	–
θ_1	$kg\,m^{-3}$	The volumetric water content for maximizing Evaporation	
θ_2	$kg\,m^{-3}$	The volumetric water content for wilting point	–
d_s	m	Soil depth	–
ρ_w	$kg\,m^{-3}$	Density of water	1000
$R_{lc,soil}$	$mol\,m^{-2}\,s^{-1}$	Soil longwave radiation	–
I_{soil}	$W\,m^{-2}$	Solar radiation on soil	–
θ_i	$kg\,m^{-3}$	The volumetric water content of the ith day	–
ρ_{va}	kPa	Vapor pressure deficit	–
HO_{soil}	$kg\,m^{-3}$	Saturated humidity of the air at the soil surface	–
HS_{soil}	$kg\,m^{-3}$	Humidity of the air at the soil surface	–
h_{soil}	m	Water pressure head	–
λ	W/(m °C)	Thermal conductivity for the soil surface	–
G_{soil}	$W\,m^{-2}$	Soil heat flux	–